

# Computational Study of Fatigue Fracture in Rivet Housing of an Aeronautical Aluminum Alloy 7075-T6

J. R. S. Moreno<sup>\*</sup>; C. Ribeiro; E. M. Junior

Mechanical Engineering Department /UTFPR - CP.  
Av. Alberto Carazzai, 1640 - Cep: 86300-000, CornélioProcópio-PR, Brasil.  
<sup>\*</sup>joaosartori@utfpr.edu.br;

**Abstract**—This article describes computerized traction testing through the ANSYS software in aircraft materials, aluminum 7075-T6, which leads to variations of the strength limits with the stress concentration factor in the rivet cavity. However, was performed with a change in the radius of transition from the head to the body of the rivet in order to alleviate the stress concentrations within the rivet bore and improve the strength of the part by 5.25% with no relevant change in part displacement. The fatigue strength limit was higher in the samples without of the burr operation, observing that the geometric trunk of the section generated a decrease of 18.27% in the maximum plate stresses, with better uniformity in the tension distribution of the rivets, with a displacement of 3.125% and a minimum equivalent stress of 2.39% and a maximum of 24%, justifying the cause of the fracture in the riveting region.

**Keywords**— Aluminum Alloy 7075-T6, ANSYS Software, Fatigue Strength, Rivets.

## I. INTRODUCTION

Technology in this industry is growing every year and one of the main focuses of research on aircraft is in relation to its weight, since fuel consumption is directly linked to the weight of the airplane. Therefore, a reduction of this aspect would entail a more competitive price of tickets since fuel expenses would be optimized.

The importance of reducing the weight of aircraft is noticeable, so they need to be the lightest and most durable, built of materials with high mechanical strength, so the use of aluminum in aeronautics has become essential because of its advantage in comparison to other materials when it comes to the relation weight as a function of the resistance [1].

These materials have as a positive point the resistance to corrosion and electrical and thermal conductivity, have good machinability and be a fragile material, yet all these characteristics do not deprive it of suffering fractures, particularly fatigue fractures when the efforts that the aircraft are submitted are so oscillating, whether due to loading, pressurizing or even the external environment

that is exposed.

In the study of Aluminum 7075 - T6 you can see a great range of benefits, compared to other materials, it admits thermal treatments, is of excellent toughness, weldable and recyclable in the general industrial environment.

Used in the manufacture of aircraft structure and other requirements of high strength, strong corrosion resistance of the high stress structure, such as aircraft, under the wing panel, stringer frame, etc.. After solution treatment, good plasticity, heat treatment strengthening effect is particularly good, in 150°C high strength and low temperature strength particularly good, poor welding performance, stress corrosion cracking, double aging can improve the resistance to SCC.

As mentioned above, its choice for the aeronautical industry is based mainly on its weight versus resistance ratio, where in Table 1 we can see some physical and mechanical properties of this material.

The plate used in the study is riveted with five rivets in a linear form with a center-to-center distance of 28.6 mm each, the rivets are of HI-LITE (HL) type made with a titanium alloy with 6% aluminum and 4% vanadium, produced by *HI-SHEAR Company* a subsidiary of *LISI S/A Aeronautical*, automotive and medical supplement development company, its activity is focused on fasteners of all kinds.

Table.1: Mechanical and Physical Properties of Aluminum Alloy 7075-T6

Mechanical and Physical Properties	Unit Metric	Unit English
Tensile strength	572 MPa	83000 Psi
Elasticity limit	503 Mpa	73000 Psi
Elongation until rupture	11%	11%
Modulus of elasticity	71.1 GPa	10400 Ksi
Resistance to fatigue	1595 MPa	23000 Psi

The plate used in the study is riveted with five rivets in a linear form with a center-to-center distance of 28.6 mm each, the rivets are of HI-LITE (HL) type made with a titanium alloy with 6% aluminum and 4% vanadium,

produced by *HI-SHEAR Company* a subsidiary of *LISI S/A* Aeronautical, automotive and medical supplement development company, its activity is focused on fasteners of all kinds.

The HI-LOK rivets, abbreviated to HL, are not ordinary rivets and yes created by the *HI-SHEAR Company* and have according to the company the combination of the

benefits of a rivet with those of a threaded screw.

The HL (HI LOK) has quick and easy installation mainly compared to a rivet or bolt, where its fastening necklace, as shown in Figure 1, has an excess of material that serves as a torque regulator so that the thread does not crush, and the HL can be fixed in the correct mode.

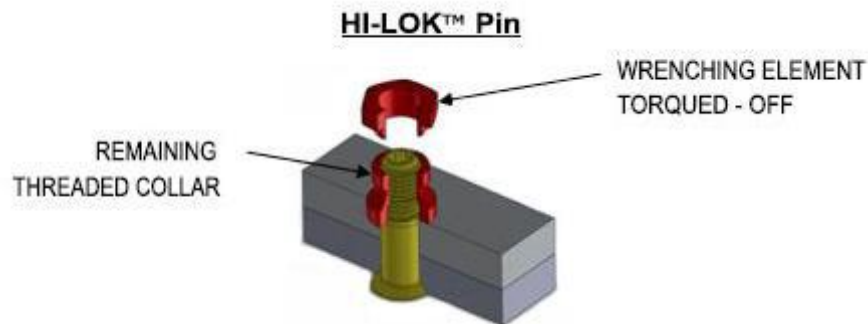


Fig.1: Rivet torqued control and pressing systems [2]

The HL compared to the other rivet models, and has a smaller working area section and therefore a shorter transition area enters the rod and the load bearing segment, with optimized transition from working area to the screw and considerably increasing the fatigue resistance.

HL type rivets account for 85% of aircraft structural joints according to *LISI S/A Company*, combining high strength materials and innovative design.

The research and development of technologies in this area are of extreme importance seeing that the current processes are becoming obsolete, and details become very important in the structural and behavioral analysis of the structures, which led this work to accurately analyze

fatigue fracture behavior of the 7075-T6 aluminum riveted with and without the scarification and burr process.

The installation of the fastening rivets involves milling and cold expansion of the main hole to the limit of fatigue crack growth is due to the compressive zone transmitted to the cold expansion orifice [3]

## II. MATERIALS AND METHODS

The test specimen (CP) used in the experimental tests is in sheet form with a useful area of 4278.24 mm<sup>2</sup> and with 5 centered and aligned rivets whose CP dimensions are shown in Figure 2 and the rivet housing in Figure 3 .

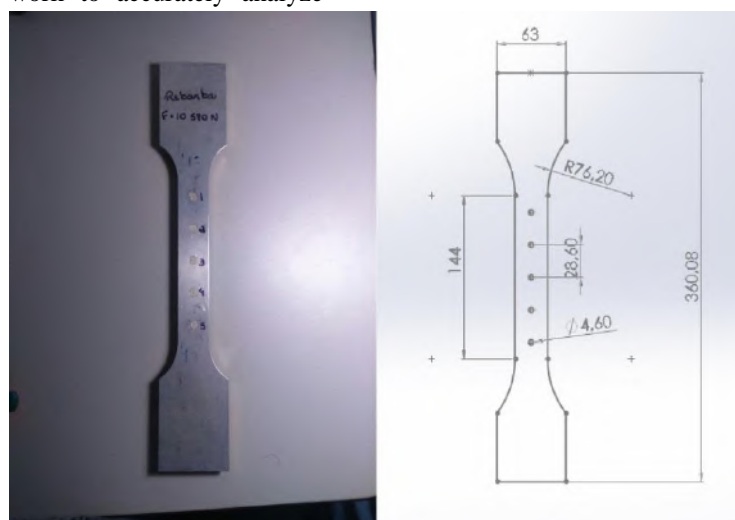


Fig.2: Type of specimens and dimensions according to norm NBR7549/2008

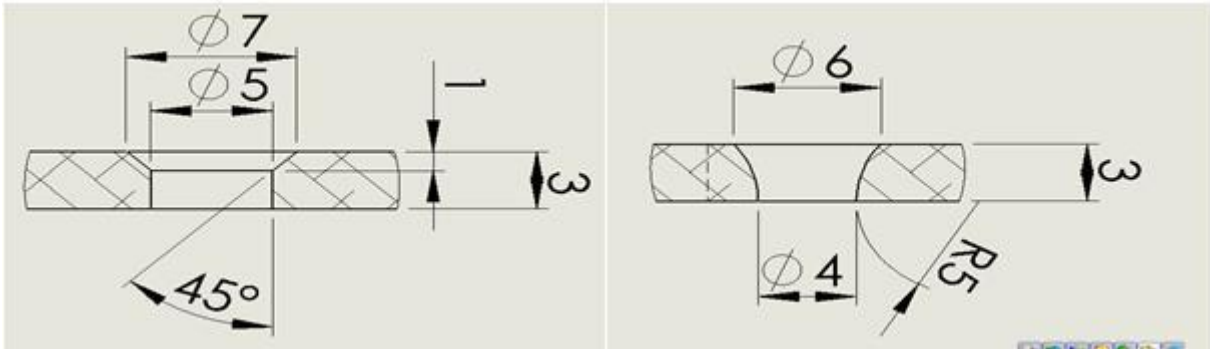


Fig.3: Specimens with the details of rivets housing reaming with dimensions in mm

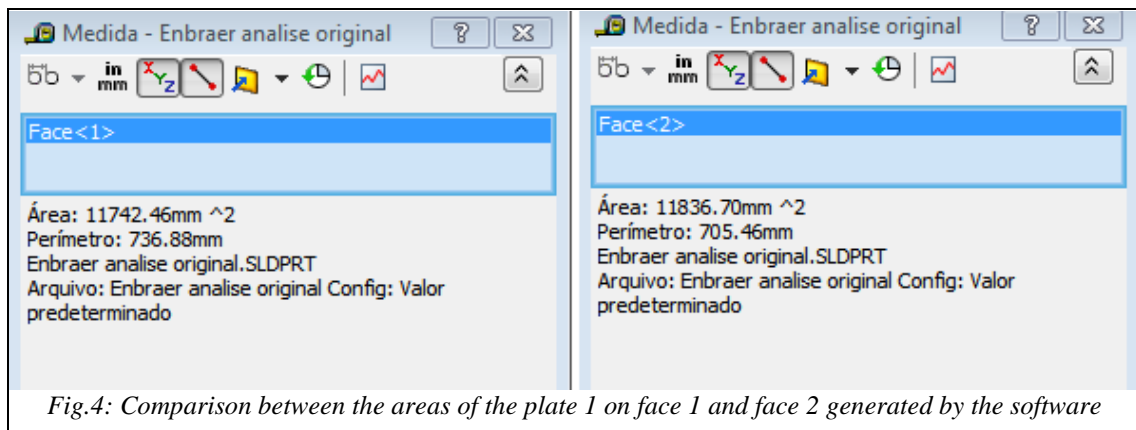


Fig.4: Comparison between the areas of the plate 1 on face 1 and face 2 generated by the software

On the right in Figure 4 we have the measurements on the plate currently used and to its left the measures to be proposed for better distribution of stresses in the plates. The HST11 6 rivet is from the Hi-Lite family as shown

previously, it is composed of 6% aluminum and 4% vanadium and 90% titanium, this material has the following mechanical properties located in Table 2 [4].

Table.2: Properties of Ti-6Al-4V Aluminum Alloy

Mechanical and Physical Properties	Unit Metric	Unit English
Tensile strength	950 MPa	138000 Psi
Elasticity limit	880 MPa	128000 Psi
Elongation until rupture	14%	14%
Modulus of elasticity	113.8 GPa	16500 Ksi
Resistance to fatigue	240 MPa	34800 Psi

### Computational analysis of the plate

After previous behavior of the plates by laboratory traction test, a computational test was performed for a better understanding of the isolated components, where the specific plate 1 (in faces 1 and 2) was studied because of the presence of rupture characteristics and concentration of loads with higher incidence, certainly due to its geometry presenting area difference between its upper and lower areas, since the geometry of the housing bore section of the rivet showed change, according to

Figure 5.

The software computational test was done by applying a fixed geometry to one of the faces of the plate and applying a load of  $1 \times 10^6$  N on the opposite face of the fixed geometry applied as shown in Figure 6. [5]

The computational analyzes were performed on the upper plate of the assembly referred to herein as plate 1 and the lower plate as plate 2 to facilitate discussion of the results obtained.

Loadname	Image Plate 1	Loadspecification	
Force-1		Local Type: Value:	1 face Normal force 100000 N

Fig.6: Demonstration of the force applied in the specimen

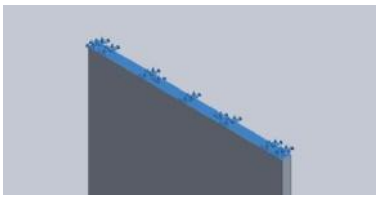
Fixing accessory	Fixture Attachment Image	Fixture accessory details		
Fixed-1		Local: Type:	1 face(s) Fixed Geometry	
Forças resultantes				
Components	X	Y	Z	Resultant
Reaction force(N)	-0.308655	99976.8	6.90748	99976.8

Fig.7: Demonstration of the type of fixation in the specimen


Mesh Information	
Type of mesh	Solidmesh
Used knit generator:	Mesh based on curvature
Jacobian Points	4 Points
Maximum element size	0 mm
Minimum element size	0 mm
Quality of the mesh	High
Total nodes	16424
Total elements	8462
Maximum proportion	6.1643
<p>Nome do modelo: Enbraer_analise original                      Nome do estudo: Estudo 1                      Tipo de malha: Malha sólida</p> 	

Fig.8: Mesh models generated by the software.

The study was based on a mesh of the solid mesh type, according to data and Figure 7, with mesh generator based on curvature, 4 Jacobian points, maximum and minimum size of elements = 0 mm, total nodes 16424, total elements 8462, maximum proportion 6,1643,% of elements with proportion <3 = 98 and completion time of the mesh = 00:00:02[6].

After the measurements of the test body and HL were taken, they were drawn in the SOLIDWORKS where the first computational tests of tensile strength were made to

generate real data of the transition part of the rivet head and the body, which was the region of greatest fragility [7].

### III. RESULTS AND DISCUSSIONS

In Figure 9, the maximum and minimum stress points of the VON MISES are determined by the software and shown on the plate for better understanding, however in Figure 10 are shown the maximum and minimum points of the resulting displacement - URES.

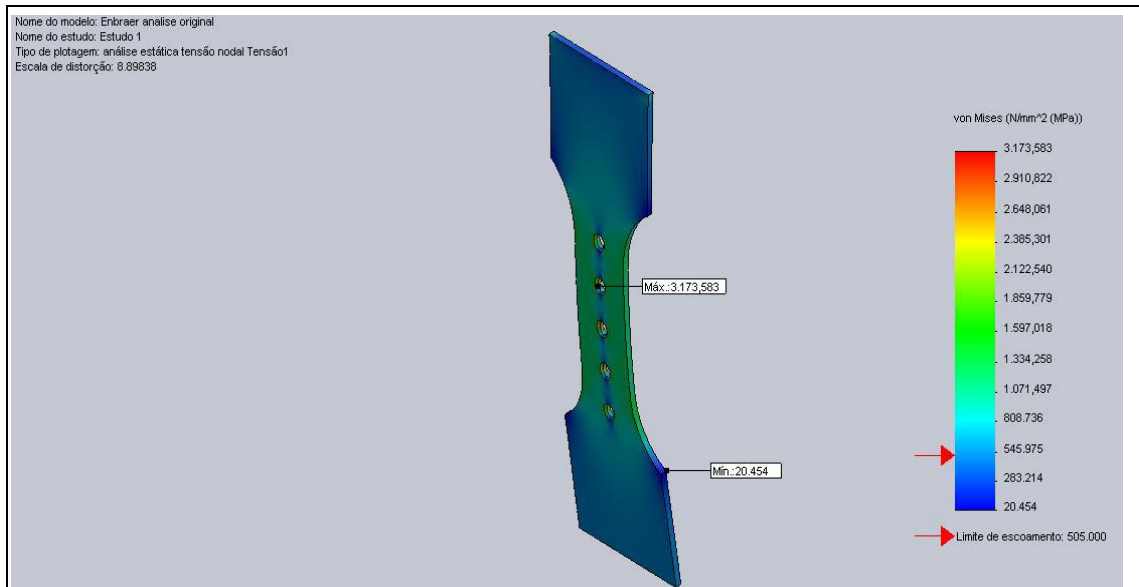


Fig.9: Points of concentration of maximum and minimum stresses of VON MISES in the computational study

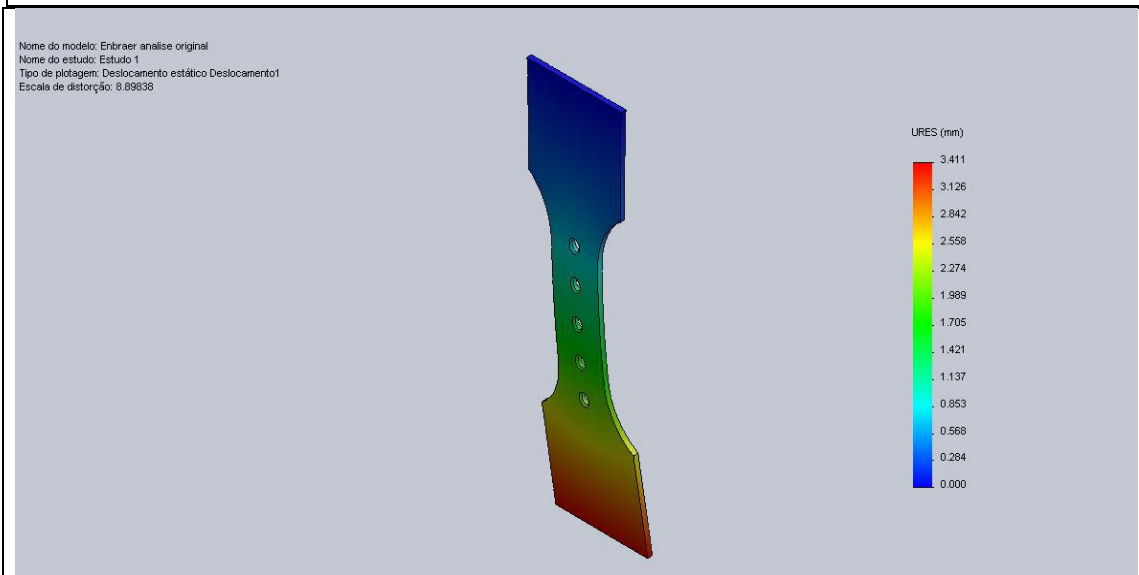


Fig.10: Displacement resulting in URES

In turn in the Figure 11 we have the points of maximum stress concentration also showing 6082.198 MPa, the yield strength that showed 505 MPa. In this image, it is noticed that the tension concentration was inside the hole where the fifth rivet is housed, in Figure 8 with the hole highlighted, we can see where the tension was

concentrated [8].

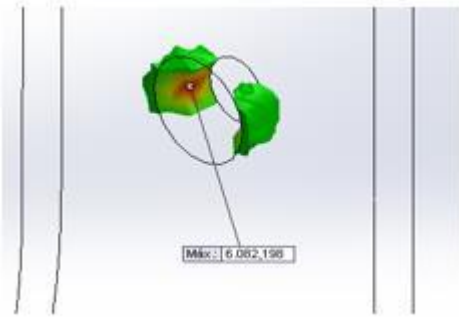


Fig.11: Point of greatest stress concentration

The point highlighted in this figure is a "living corner" produced by the shape of the rivet, it is in the transition from head to body, where there is a radius of 0.75mm, but it is not able to relieve concentration at this point

When we analyze the ray, we can see that it only exerts a smooth transition between the head of the rivet and the body and does not help in a better distribution of force and less concentration, so acting on this ray can represent much more expressive results. Thus, by analyzing different rays the following result is shown in Figure 9.

As the test demonstrates, with the change of radius to the value of 0.39, there was an increase of 319.503 MPa in the tensile strength somewhat around 5.25% increase, something much larger than the 1.76% of the transition radius. [9,10]

Complementary to the computational tests, fatigue tests were carried out on the test bodies at the Institute Technological Aeronautics (ITA- BRAZIL) at the request of EMBRAER, the company interested in the

study, which allowed us to verify that the fatigue strength limit of the material was maximum of 16.6 Ksi at  $2 \times 10^6$  cycles with burr operation and maximum of 19.1 Ksi at  $2 \times 10^6$  cycles without burr operation.

For comparative purposes, the maximum tensions and fatigue strength of the respective specimens [11] were highlighted in Table 3 and Table 4.

Table.3: Fatigue test of the CP with burr operation

Net Stress(Ksi)	Maximum Loading (N)	Cycles
37.017	20260	20919
16.564	9130	2000000

Table.4: Fatigue test of the CP without burr operation

Net Stress (Ksi)	Maximum Loading (N)	Cycles
36.6	20260	72081
19.1	10580	2000000

On the other hand, in Figure 12, the equivalent ESTRN equivalent maximum and minimum points are shown on the plate for a better understanding. Equivalent strain (ESTRN) is defined on the X, Y, Z axes as:

$$ESTRN = 2 [(\epsilon_1 + \epsilon_2) / 3]^{(1/2)}$$

Where:

$$\epsilon_1 = 0.5 [(\epsilon_{PSX} - \epsilon^*)^2 + (\epsilon_{PSY} - \epsilon^*)^2 + (\epsilon_{PSZ} - \epsilon^*)^2]$$

$$\epsilon_2 = [(GM_{XY})^2 + (GM_{XZ})^2 + (GM_{YZ})^2] / 4$$

$$\epsilon^* = (\epsilon_{PSX} + \epsilon_{PSY} + \epsilon_{PSZ}) / 3$$

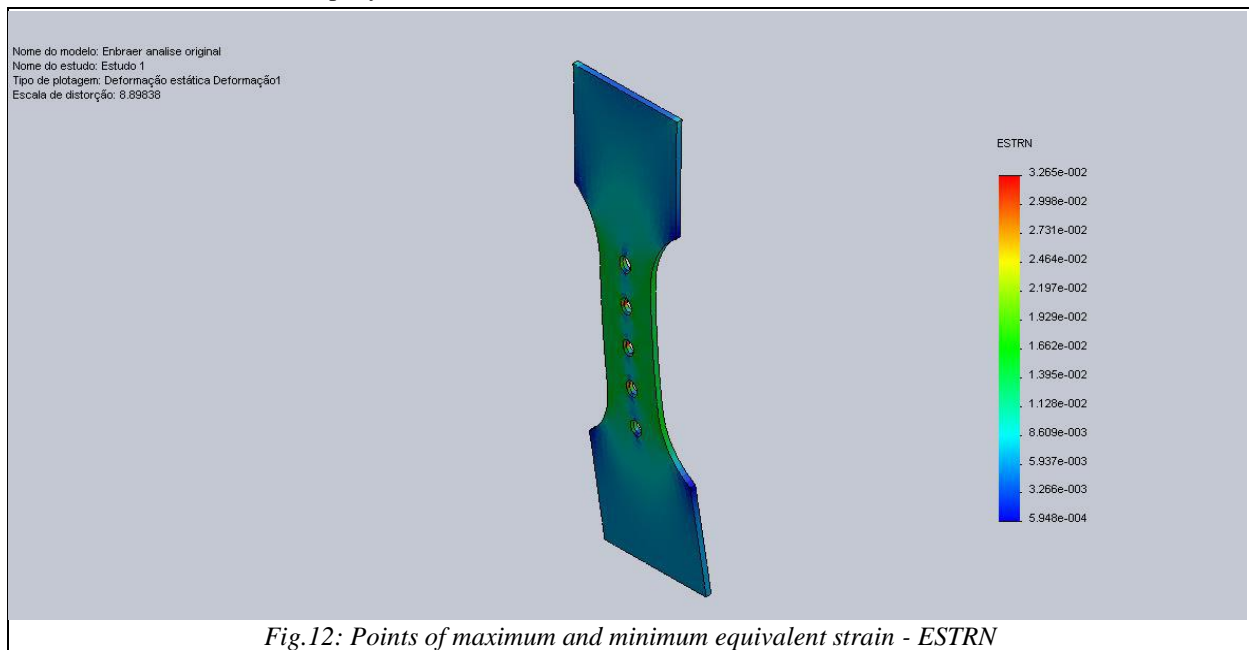


Fig.12: Points of maximum and minimum equivalent strain - ESTRN

Thus the results obtained from the values for this new geometry proposition are presented in table 5:

Table.5: Results of the analysis and its positions in the mesh (Proposed plate 1)

Type	Values	Situation
VON MISES Stress	20.4380 N/mm <sup>2</sup> (MPa)	Node: 174
	2594.81 N/mm <sup>2</sup> (MPa)	Node: 16435
URES: Resultingdisplacement	0,0 mm	Node: 94
	3.52 mm	Node: 193
ESTRN: Equivalentdeformation	0.000609347	Element: 5877
	0.0238112	Element: 4629

The test specimens of the fatigue test behaved as expected and predicted in the computational traction tests where the rupture occurred at that point by the charge concentration due to the geometry of the section of the hole of the upper plate as shown in Figure 13, thus there being thus a "tearing" of the plate.

Results of these tests extend information previously reported from tests on unnotched specimens and tests on specimens more severely notched and afford data on the variation of fatigue-strength reduction with notch severity.



Fig.13: Top and bottom view of the failure.

Under rotating bending fatigue tests the high stress zones are located at the fracture surface perimeter and decrease to the fracture surface center: the size of grooves decreases from fracture surface perimeter to the center [12]. Furthermore, for this type of specimen the center of fracture surface is characterized by fast crack growth zone

where the plastic deformation is small or zero. This rupture occurred at that point by the charge concentration due to the geometry of the section of the bore of the upper plate as shown in Figure 14, thus there being a "tearing" of the plate as shown in Figure 13

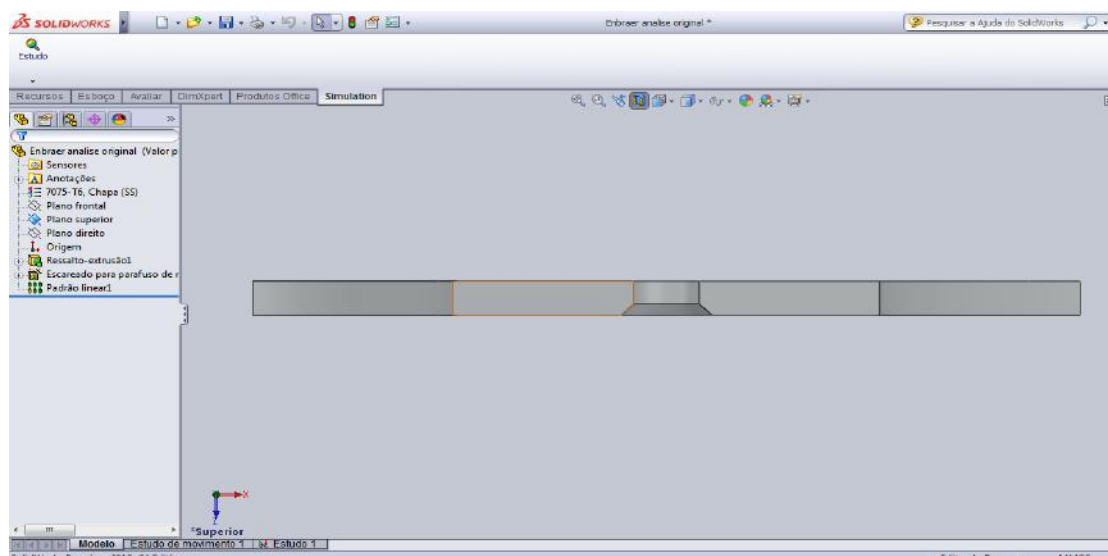


Fig.14: View of the geometry of the upper plate hole section

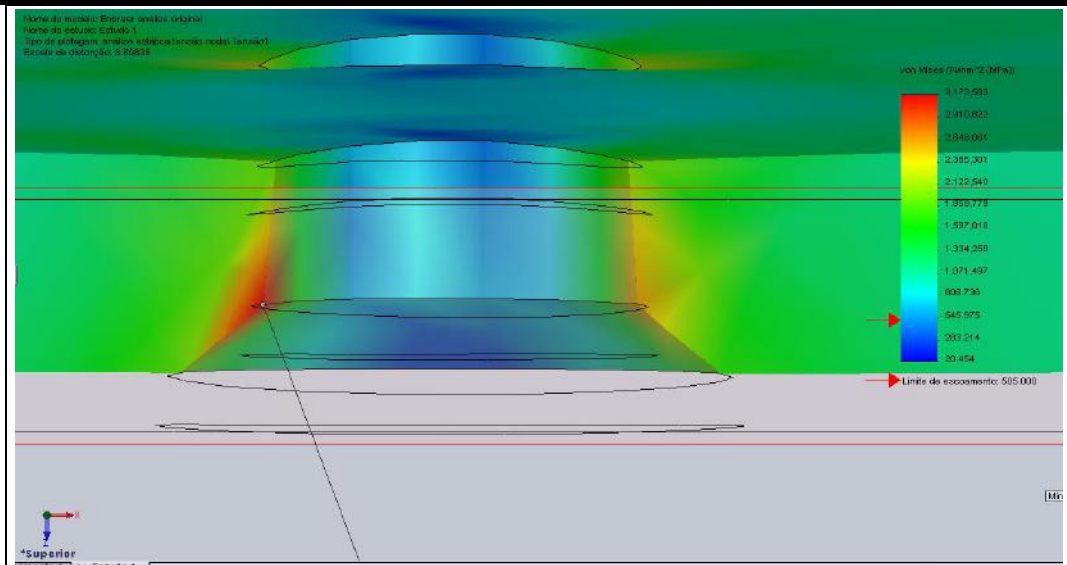


Fig.15: Defined configurations for the rivet housing in better geometric for structural conditions to section of the original housing

The fatigue cracking growth is associated with the growth of cracks in the riveted fracture mechanics. In turn, small cracks and grain size limitations in the microplastic regions, cause deceleration gradients and consequent slower cracking evolution [13,14].

The stress intensity is used to predict the stress state near the hole and crack tip caused by the applied loading; as the crack tip radius is effectively zero, the stresses at the crack tip would be infinite[15-16]

After changing the geometry of the housing section of the

rivet there was a reduction of approximately 18.27% in the maximum stresses in the plate plus a better uniformity in the stress distribution in the housings as shown in Figure 15 and 16, whereas the displacement only had an increase of 3.125% and the minimum equivalent strain of 2.39% and the maximum of 24%.The stress distribute drafts of the riveted plates obtained so that it is convenient to check the bending strength of the root of the hole and the fatigue contact strength of the union faces[16].

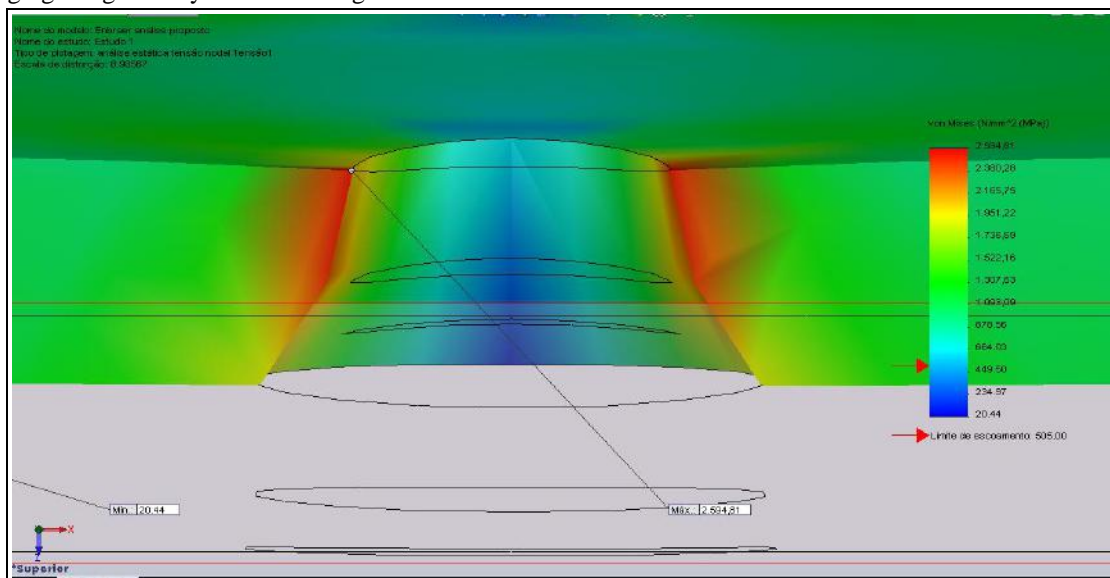


Fig.16: Defined configurations for the rivet housing in better geometric for structural conditions to section of the proposed housing

#### IV. CONCLUSIONS

Based on the results and computational techniques used in this work, the computerized tensile test with an intermediate level of certainty, it is determined that with a change in the radius of transition from the head to the body of the rivet, we can relieve the concentration of

tension within the rivet bore and improve the mechanical strength of the part by 5.25% without significant change in part displacement. However in the fatigue tests performed the work behaved as expected with fractures in the vicinity of the HL, but with the reaming operation there was a small inference on the fatigue strength.



However, the fatigue strength limit was higher in the test specimens without burr operation than the operation, noting that the geometric change of the section generated a decrease of 18.27% in the maximum stresses in the sheet, in addition to a better uniformity in the distribution of the tension in reaming of the rivets, with displacement increasing by 3.125% and the minimum equivalent strain of 2.39% and the maximum of 24%, often explaining the cause of the fracture.

#### ACKNOWLEDGMENT

This work was made possible through an interaction with the ITA - Aeronautical Technological Institute/EMBRAER that helped us in the interactions of aircraft component fixation projects and provided us with data for observations and analyzes. We should also thank the UTFPR - Federal Technological University of Paraná that subsidized us for the works.

#### REFERENCES

- [1] Matweb.; Aluminum 7075-T6; 7075-T651  
:<<http://www.matweb.com/search/DataSheet.aspx?MatGUID=4f19a42be94546b686bbf43f79c51b7d&c ck=1>>. 2016
- [2] Lisi. HI-Lite PIN. <<http://www.lisi-aerospace.com/products/fasteners/externally-threaded/pin/Pages/hi-lite.aspx#criteriaGrouping>>. 2016
- [3] Fltlt B Krutop, F.A.B.(2008), *P-3C Orion Aircraft Structural Integrity Management Plan.*, DGTA: Canberra, Australia
- [4] Roy, P., Sarangi, S.K., GHOSH, A.(2009), Chattopadhyay, A.K., 2009. Machinability study of pure aluminium and Al-12% Si alloys against uncoated and coated carbide inserts. *Int. J. Refract. Metal Hard Mater*; 27, .535-544
- [5] Sousa, M., Silva, M., Sousa, J., Barrozo, M., Machado,Á (2013).;Relação entre as Propriedades Mecânicas das Ligas de Alumínio e o Grau de Recalque<<http://www.abcm.org.br/anais/cobef/2013/PDFS/COBEF2013-0042.PDF>>
- [6] Oh, S. I. And Kobayashi, S. (2010).; Work ability of Aluminum Alloy 7075-T6 in upsetting and Rolling; *Journal Engineering Industrial*, 98(3), 800-806, doi:10.1115/1.3439032
- [7] Zehsaz, M., Rahmatfam, A., Rahmatfam, M. (2017) ; Experimental Determination of Aluminum 7075-T6 Hardening Parameters to Predict Thermal Ratcheting *Proceedings of the 7th International Conference on Mechanics and Materials in Design*Albufeira/Portugal.
- [8] Harrison, T. J. , Janardhana,M. And Clark, G. (2011); Differing microstructural properties of 7075-T6 sheet and 7075-T651 extruded aluminium alloy; *Procedia Engineering*; 10,.3117-3121
- [9] ABNT; Calibração De Força Dinâmica No Ensaio De Fadiga Uniaxial (2016) – Disponível em: <<http://www.abnt.org.br/noticias/4641-calibracao-da-forca-dinamica-no-ensaio-de-fadiga-uniaxial>>
- [10] Whaley, R. E. (1962) ; Fatigue and static strength of notched and unnotched aluminum-alloy and steel specimens. *Experimental Mechanics*;2(11), 329–334
- [11] Dong, K. (2015) "Simulation Study on Aluminium Alloy 7075-T6 Welding Based on ANSYS Software", *Applied Mechanics and Materials*, 727-728, 30-33,
- [12] Domínguez Almaraz G.M., Mercado Lemus V.H., Mondragón Sánchez M.L.(2009), Crack Initiation and propagation on AISI-SAE stainless steel 304 under rotating bending fatigue tests and close to elastic limit, *Crack Paths*, Vicenza, Italy: 961-968
- [13] Yaodong, G. and Xue, H.(2010); Welding Simulation based on ANSYS Element Life and Death Technology [J], *Hot Working Technology*, .39 (7), 120-126
- [14] Chen, Dyi-C., You, S., and Gao, Fu-Y. (2014); Analysis and Experiment of 7075 Aluminum Alloy Tensile Test; *Procedia Engineering*, 81, 1252-1258
- [15] Zhao, J., Liu, J. And Zhao, Q. (2012), A method for stress intensity factor calculation of infinite plate containing multiple hole-edge cracks. *International Journal of Fatigue*, 35(1), 2-9
- [16] Noda, N.A. (2012), Stress intensity factors for an edge interface crack in a bonded semi-infinite plate for arbitrary material combination. *International Journal of Solids and Structures*, 49(10), 1241-1251